

Generation of potential energy curves for the $X^1\Sigma_g^+$, $B^1\Delta_g^+$, and $B'^1\Sigma_g^+$ states of C_2 using the effective valence shell Hamiltonian method

Rajat K. Chaudhuri^{a)}

Indian Institute of Astrophysics, Bangalore-560034, India

Karl F. Freed

The James Franck Institute and Department of Chemistry, University of Chicago, Chicago, Illinois 60637

(Received 3 January 2005; accepted 2 February 2005; published online 20 April 2005)

Calculations of the ground and excited state potential energy curves of C_2 using the third-order effective valence Hamiltonian (H_{3rd}^v) method are benchmarked against full configuration interaction and other correlated single-reference perturbative and nonperturbative theories. The large nonparallelity errors (NPEs) exhibited even by state-of-art coupled cluster calculations through perturbative triples indicate a serious deficiency of these single-reference theories. The H^v method, on the other hand, produces a much reduced NPE, rendering it a viable approximate many-body method for accurately determining global ground and excited state potential energy curves/surfaces. © 2005 American Institute of Physics. [DOI: 10.1063/1.1879812]

I. INTRODUCTION

The most direct approach for assessing the accuracy and reliability of approximate quantum chemical many-body methods is by comparing predicted quantities against the exact solution of the electronic Schrödinger equation in a given basis set, i.e., by comparing with the full configuration interaction (FCI) treatment in which all possible Slater determinants of the appropriate symmetry and spin are generated from the basis. Unfortunately, FCI calculations are usually only feasible for small molecules with modest basis sets as the number of Slater determinants grows factorially with the number of basis functions and/or electrons. Although the FCI method is generally impractical as a general computational scheme, it provides the best benchmark for assessing the reliability and deficiencies of theoretical methods. Moreover, the information gained from comparisons with FCI calculations can be utilized to design and improve reliable many-body methods for treating difficult systems, such as those involving bond breaking reactions and/or open-shell excited states.

Abrams and Sherrill¹ have recently tested the accuracy of single-reference perturbative and nonperturbative methods in treating the C_2 bond breaking reaction using FCI calculations for a 6-31G* basis set. These benchmark tests compare FCI potential curves for the $X^1\Sigma_g^+$, $B^1\Delta_g^+$, and $B'^1\Sigma_g^+$ states of the C_2 molecule with those predicted by coupled cluster (CC) methods²⁻⁵ and its variants.⁶⁻¹⁰ Their benchmark calculations for this very nontrivial system demonstrate that even state-of-art CC methods with perturbative triples (using an unrestricted Hartree-Fock reference function) are incapable of providing accurate potential curves for C_2 . Abrams and Sherrill also show that almost all correlated many-body methods that are based on a restricted Hartree-Fock (RHF) reference exhibit large nonparallelity errors (NPE) even for

the ground $X^1\Sigma_g^+$ state because the single-reference theories are not designed for bond breaking reactions. The unrestricted Hartree-Fock (UHF) reference CC calculations yield qualitatively correct potential energy curves but suffer from the usual quantitative NPE inaccuracies.

In this article, we compare the three potential energy curves of C_2 generated by the effective valence shell Hamiltonian (H^v) theory with those from the FCI and other correlated treatments. Extensive theoretical studies¹¹⁻²⁰ document the H^v formalism, its conceptual advantages, the computational algorithms for evaluating atomic and molecular properties, and the higher-order convergence behavior of the method.²¹ The present work demonstrates that the H^v method produces highly reliable and uniformly accurate potential curves of C_2 , whereas virtually all single-reference correlated theories fail near the dissociative regions. The calculations once again underscore the greater suitability of multireference theories, such as the H^v method, for modeling bond-breaking reactions, even in doubly excited electronic states.

As the details of the H^v are extensively discussed in some of our earlier communications, we only outline the essential features of this method in the next section, with the calculations described in the following section.

II. THEORETICAL APPROACH

The effective Hamiltonian method (H^v) belongs to the “perturb then diagonalize” variety of multireference many-body perturbation theories (MR-MBPT). H^v theory also differs from MR-MBPT methods that are based on Möller-Plesset (MP)-type partitionings in the choice of unoccupied valence orbitals and their energies. In the H^v theory, the unoccupied valence orbitals and their energies are determined as improved virtual orbitals from a V^{N-1} Fock operator to more appropriately describe low lying excited states in first

^{a)}Electronic mail: rkchaudh@kffl.uchicago.edu

order and thereby to minimize the residual left for the perturbation expansion. The zeroth-order Hamiltonian $H^{(0)}$ is defined as

$$H^{(0)} = \sum_c |\phi_c\rangle \epsilon_c \langle \phi_c| + \sum_v |\phi_v\rangle \bar{\epsilon}_v \langle \phi_v| + \sum_e |\phi_e\rangle \epsilon_e \langle \phi_e|, \quad (2.1)$$

in terms of the core (c), valence (v), and excited (e) orbital energies ϵ_c , $\bar{\epsilon}_v$, and ϵ_e , respectively. The occupied orbitals in the ground $X^1\Sigma_g^+$ RHF approximation are used as the core and “occupied” valence orbitals, while the remaining “unoccupied” valence orbitals are improved virtual orbitals. The two core orbitals are doubly occupied in P space, while eight valence orbitals form the complete active space (CAS) defining the rest of the P space as described below.

Perturbative convergence²¹ is enhanced by evaluating the forced degeneracy valence orbital energy $\bar{\epsilon}_v$ from the original set of valence orbital energies ϵ_v by the democratic averaging,

$$\bar{\epsilon}_v = \frac{\sum_v \epsilon_v}{N_v}, \quad (2.2)$$

with N_v representing the number of valence orbitals in the CAS spanned by the set of valence orbitals ϕ_v . (For further details, see Ref. 11).

Calculations indicate that near the ground-state equilibrium internuclear separation ($R_{CC}=1.25$ Å), the ground-state wave function of C_2 is dominated by the $|(core)2\sigma_g^2 2\sigma_u^2 1\pi_x^2 1\pi_y^2\rangle$ and $|(core)2\sigma_g^2 1\pi_x^2 1\pi_y^2 3\sigma_g^2\rangle$ configuration state functions (CSFs). At the same geometry, the $B^1\Delta_g$ state is dominated by $|(core)2\sigma_g^2 2\sigma_u^2 1\pi_x^2 3\sigma_g^2\rangle - |(core)2\sigma_g^2 2\sigma_u^2 1\pi_y^2 3\sigma_g^2\rangle$ CSF, while the $B'^1\Sigma_g^+$ state has these same two CSFs but with the same sign. Note that both the $B^1\Delta_g$ and $B'^1\Sigma_g^+$ states are doubly excited with respect to the ground $X^1\Sigma_g^+$ state, thereby posing added computational difficulties for many correlated methods.

The choice of reference space plays a central role in all MR-MBPT methods. This choice is also the most difficult portion of all multireference perturbative methods as it can affect the accuracy of both spectroscopic constants and global potential energy surfaces (or curves for diatomic molecules). While the choice of reference space is fairly straightforward near the Franck–Condon bonding region, matters become more complex as the system approaches the dissociative region where the reference space must properly describe the bond fragmentation. The H^v approach overcomes these difficulties in a relatively straightforward fashion by constructing a reference space that satisfies both sets of conditions.

Because the carbon atom $2s$ and $2p$ orbitals become quasidegenerate upon dissociation, the $2s$ and $2p$ orbitals of each carbon atom should be included in the CAS to describe the bond fragmentation process in C_2 . (Note that the C_{1s} orbital is kept frozen in the FCI (Ref. 1) and all other calculations.) Figure 1 presents ground-state RHF orbital energies for the four occupied ($2\sigma_g, 2\sigma_u, 1\pi_u$) and four low-lying unoccupied ($3\sigma_g, 3\sigma_u, 1\pi_g$), orbitals of C_2 as a function of the C–C internuclear distance. Figure 1 shows that near the

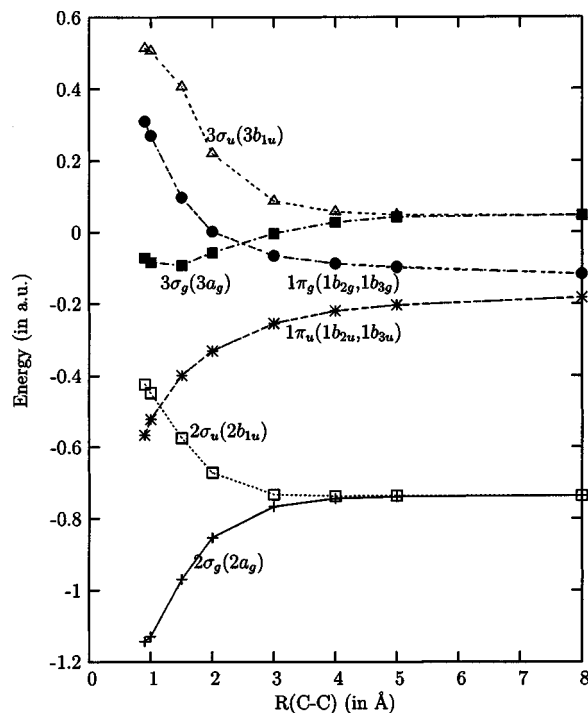


FIG. 1. RHF orbital energies (in a.u.) of C_2 vs. R_{C-C} (in Å).

Franck–Condon region (~ 1.25 Å), the occupied $1\pi_u$ and $2\sigma_u$ orbitals are quasidegenerate, while as the system approaches the dissociative region, $\epsilon_{2\sigma_s} - \epsilon_{2\sigma_u} \rightarrow 0$, making these two orbitals degenerate. The unoccupied orbitals $3\sigma_g$, $1\pi_g$, and $3\sigma_u$ also exhibit similar trends. Based on these arguments, all eight orbitals must be clearly included in the CAS to model the bond breaking reactions of C_2 .

Figure 2 compares the ground $X^1\Sigma_g^+$ state potential curve of C_2 as computed using the third-order H^v (H_{3rd}^v) method

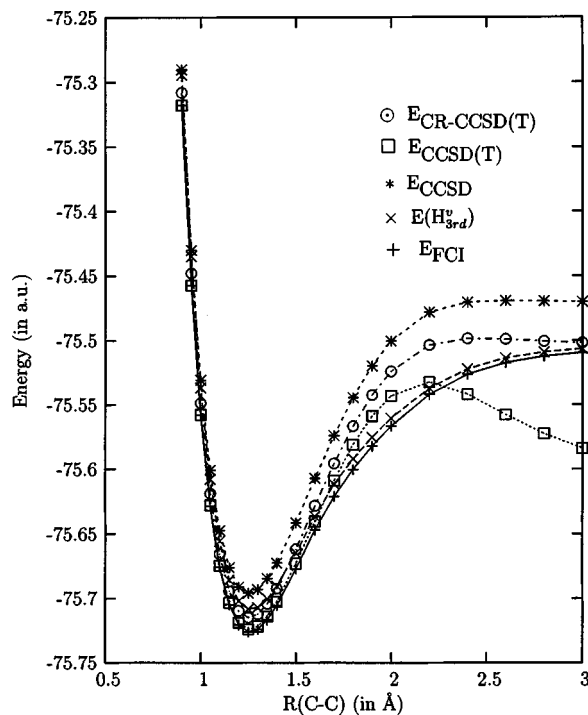


FIG. 2. $X^1\Sigma_g^+$ state energy (in a.u.) of C_2 vs. R_{C-C} (in Å).

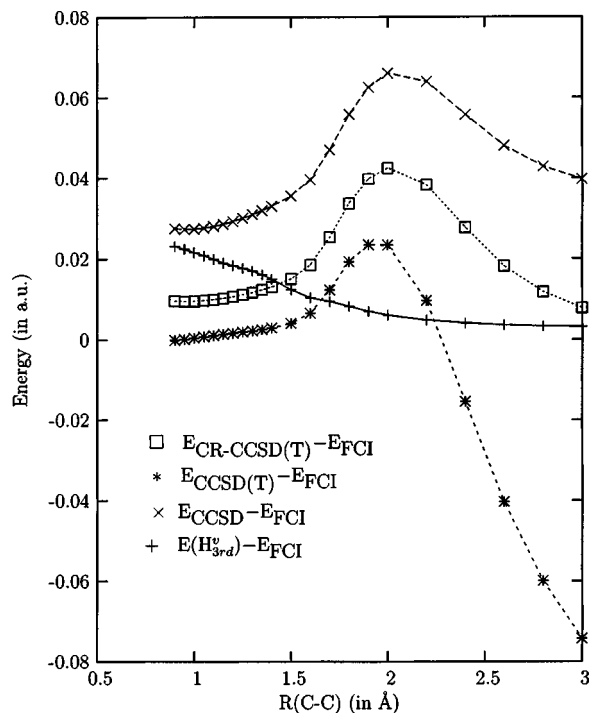


FIG. 3. $E_{\text{theory}} - E_{\text{FCI}}$ for $X^1\Sigma_g^+$ state of C₂ vs. $R_{\text{C-C}}$ (in Å).

with the FCI and with single-reference based CC calculations. The potential curve evaluated from the CC singles and doubles with perturbative triples [CCSD(T)] fails badly upon dissociation. The CCSD(T) ground-state energy is not only nonphysically large but also falls below the FCI. However, this type of behavior of the CCSD(T) potential curves near the bond-breaking region is commonly observed and appears even in the bond fragmentation of the BH and HF molecules.²² The CCSD and its completely renormalized version [CR-CCSD(T)]^{7,8} yield a ground-state potential-energy curve which is qualitatively but not quantitatively correct.

The errors in all these approximate methods may be examined more critically in Fig. 3 which presents the deviation $E_{\text{theory}} - E_{\text{FCI}}$ of the computed ground-state energies from the FCI (Ref. 1) as a function of internuclear distance. In addition, Table I displays the NPEs for various approximate methods as a global measure of their accuracy, where the NPEs are defined as the difference between the maximum deviation and the minimum deviation from the FCI estimate over the entire potential-energy curve/surface. Figure 3 clearly demonstrates that the $H_{3\text{rd}}^v$ error curve is by far the flattest. (An ideal method produces a completely flat error curve.) Table I further indicates that the $H_{3\text{rd}}^v$ method yields smaller errors than all variants of single-reference CC theories and the venerable CI with singles, doubles, triples, and quadruple (CISDTQ) excitations.

We now consider the $B^1\Delta_g^+$ and $B'^1\Sigma_g^+$ excited states of C₂. Under the D_{2h} subgroup, both states belong to 1A_g symmetry. The excited $B'^1\Sigma_g^+$ and $B^1\Delta_g^+$ state energies of C₂ computed using the $H_{3\text{rd}}^v$ method are compared with the FCI (Ref. 1) and with equation-of-motion (EOM) CC treatments in Figs. 4 and 5, respectively. The NPEs for these two states are compared with those from EOM-CC calculations in Table I. The EOM-CC potential curves for the $B'^1\Sigma_g^+$ and

TABLE I. Maximum, minimum, and nonparallelity errors (in kcal/mol) with respect to the FCI for the $X^1\Sigma_g^+$, $B^1\Delta_g^+$, and $B'^1\Sigma_g^+$ states of C₂. The values in parentheses indicate the corresponding bond distance in angstroms.

State	Method	Max. error	Min. error	NPE
$X^1\Sigma_g^+$	RHF ^a	339.3 (3.00)	206.4 (0.90)	132.9
	MP2 ^a	33.8 (2.00)	-47.5 (3.00)	81.3
	CISD ^a	109.6 (3.00)	-37.0 (0.90)	72.6
	CCSD(T) ^a	14.7 (1.90)	-46.6 (3.00)	61.3
	CISDT ^a	79.7 (3.00)	24.9 (0.90)	54.8
	UHF ^a	142.4 (1.30)	93.7 (3.00)	48.7
	UMP2 ^a	61.4 (1.80)	20.7 (0.90)	40.7
	CCSDT ^a	17.3 (2.00)	-14.2 (3.00)	31.5
	CR-CCSD(T)	26.6 (2.00)	4.9 (3.00)	21.7
	UCCSD ^a	31.0 (1.80)	4.0 (3.00)	27.0
	CCSD ^a	41.4 (2.00)	17.2 (0.95)	24.3
	UCCSD(T) ^a	24.4 (1.90)	2.8 (3.00)	21.6
$B'^1\Sigma_g^+$	CISDTQ ^a	18.9 (2.40)	2.3 (0.90)	16.6
	$H_{3\text{rd}}^v$	14.5 (0.90)	1.9 (3.00)	12.6
	[1,0] Padé	5.9 (0.90)	1.9 (3.00)	4.0
	EOM-CCSD	80.9 (3.00)	35.3 (0.90)	45.6
$B^1\Delta_g^+$	$H_{3\text{rd}}^v$	14.2 (0.90)	1.7 (3.00)	12.5
	[1,0] Padé	7.3 (0.90)	1.7 (3.00)	5.6
	EOM-CCSD	95.2 (2.80)	63.9 (1.15)	31.3
	$H_{3\text{rd}}^v$	14.6 (0.90)	1.9 (3.00)	12.7
	[1,0] Padé	7.8 (0.90)	1.9 (3.00)	5.9

^aTaken from Ref. 1.

$B^1\Delta_g^+$ states lie much higher than the FCI curve as anticipated because the EOM-CC is known to provide a poor description for doubly excited states. The excited state potential energy curves produced by the $H_{3\text{rd}}^v$ method, on the other

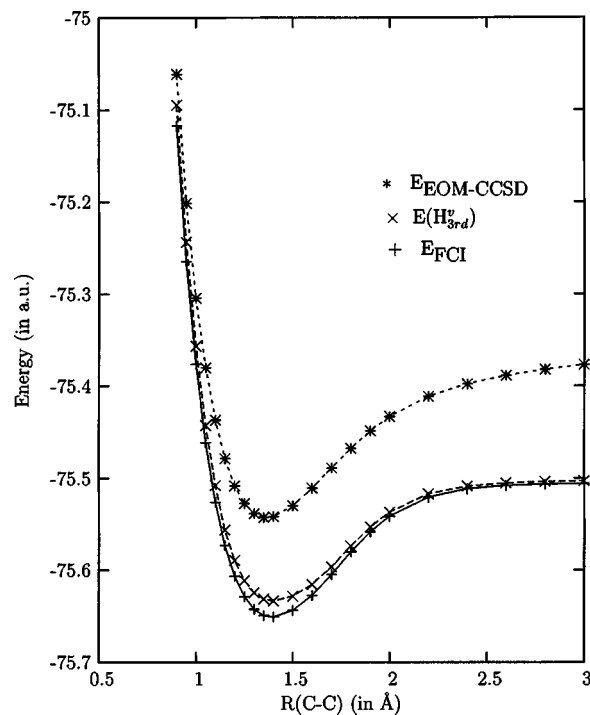


FIG. 4. $B^1\Sigma_g^+$ state energy (in a.u.) of C₂ vs. $R_{\text{C-C}}$ (in Å).

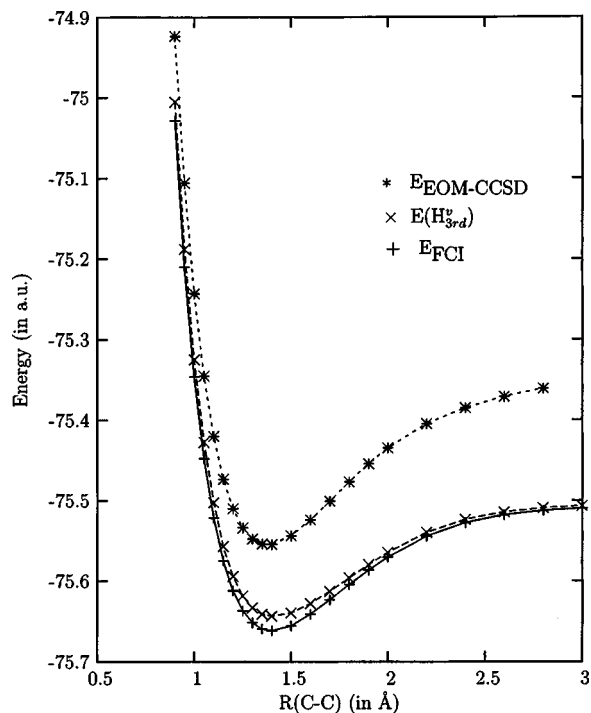


FIG. 5. $B^1\Delta$ state energy (in a.u.) of C_2 vs. R_{C-C} (in Å).

hand, are not only close to FCI but are also quite accurate. (The H_{3rd}^v NPEs for these two excited states are indeed quite small.)

Table II compares the spectroscopic constants for the ground $X^1\Delta_g^+$ and excited $B^1\Delta_g^+$ and $B'^1\Sigma_g^+$ states of C_2 computed using the H_{3rd}^v method with those from the FCI, CCSD,

TABLE II. Spectroscopic constants and vertical excitation energies (VEEs) of C_2 . Spectroscopic constants are estimated by fitting the potential energies to Morse potential. (Extra points generated near R_e for H_{3rd}^v and EOM-CCSD methods.)

Spectroscopic constants	Method	$X^1\Sigma_g^+$	$B'^1\Sigma_g^+$	$B^1\Delta_g^+$
R_e (in Å)	FCI	1.254	1.381	1.398
	CCSD/EOM-CCSD	1.254 ^a	1.361	1.375
	H_{3rd}^v	1.260	1.392	1.409
	[1,0]Padé	1.255	1.386	1.402
	FCI	5.880	3.943	4.134
D_e (in eV)	CCSD/EOM-CCSD	6.140	4.504	5.267
	H_{3rd}^v	5.482	3.542	3.727
	[1,0]Padé	5.731	3.739	3.942
ω_e (in cm^{-1})	FCI	1800	1361	1393
	CCSD/EOM-CCSD	1930 ^b	1399	1534
	H_{3rd}^v	1742	1309	1343
	[1,0]Padé	1792	1336	1372
T_e (in eV)	FCI	0.0	2.043	1.744
	CCSD/EOM-CCSD	0.0	4.168	3.840
	H_{3rd}^v	0.0	2.038	1.753
	[1,0]Padé	0.0	2.090	1.787
VEE (in eV)	FCI	0.0	2.642	2.425
	CCSD/EOM-CCSD	0.0	4.581	4.407
	H_{3rd}^v	0.0	2.552	2.343
	[1,0]Padé	0.0	2.678	2.457

^aFrom numerical CCSD optimization.

^b $\omega_e = 1906\text{ cm}^{-1}$ (from numerical CCSD optimization).

and EOM-CCSD methods. The CC treatment produces an excellent ground state equilibrium internuclear separation, while the EOM-CC equilibrium bond lengths for the excited state deviate from the FCI by 0.02 Å . The EOM-CC adiabatic (T_e) and vertical excitation energies (VEEs) and vibration frequencies (ω_e) deviate considerably (by $\sim 2\text{ eV}$, $\sim 2\text{ eV}$, and $38\text{--}141\text{ cm}^{-1}$, respectively) from the FCI. Though the CC calculations overestimate the dissociation energies (D_e) by $0.2\text{--}1.0\text{ eV}$, the results are not as poor as the treatment of the T_e and VEEs.

In contrast, the H_{3rd}^v offers uniformly accurate estimates for the T_e and VEEs. More specifically, the H_{3rd}^v errors in the equilibrium internuclear separation of $\sim 0.01\text{ Å}$ are comparable to those of the EOM-CC, while the minuscule errors in T_e of $\sim 0.01\text{ eV}$ are perhaps a bit fortuitous given the larger VEE errors of $\sim 0.1\text{ eV}$. The H_{3rd}^v errors in D_e , on the other hand, are $\sim -0.4\text{ eV}$, indicating that the bonding region is more correlated than the fragmentation region. This feature is probably also responsible for the errors in ω_e of $\sim -53\text{ cm}^{-1}$. Nevertheless, the performance of the H_{3rd}^v calculations for D_e and ω_e outshines the CC treatment.

Given the non-negligible deviation of the H_{3rd}^v calculations for D_e and ω_e from the FCI, we consider whether these may be improved by the use of [1,0]Padé resummations. Table I indicates that [1,0]Padé reduces the NPE by at least a factor of 2. (The NPE decreases from 12.6 to 4.0 kcal/mol for the ground, from 12.5 to 5.6 kcal/mol for the $B'^1\Sigma_g^+$, and from 12.7 to 5.9 kcal/mol for $B^1\Delta_g$ state of C_2 .) The [1,0]Padé improves the description of R_e slightly, corrects ω_e by $30\text{--}50\text{ cm}^{-1}$, improves D_e by $\sim 0.2\text{ eV}$ and the VEEs by $\sim 0.1\text{ eV}$, while the accuracy of T_e is degraded to a perhaps more realistic error of $\sim 0.05\text{ eV}$.

The error $E_{H_{3rd}^v} - E_{FCI}$ in Fig. 3 for the ground state decreases as R_{C-C} increases. A similar trend also emerges for the $B^1\Delta_g$ and $B'^1\Sigma_g^+$ excited states. The NPEs computed from H_{3rd}^v potential curves reflect the same trend. This behavior may be explained with the aid of Eq. (2.1) and Fig. 1. The quasidegeneracy among the CAS orbitals (see Fig. 1) increases as the system approaches the bond dissociative region. It follows that the perturbation $\epsilon_0 - \bar{\epsilon}$, which contributes to the H_{3rd}^v energy, also decreases as R_{C-C} increases. Thus, the magnitude of the perturbation diminishes, and $E_{H_{3rd}^v} - E_{FCI}$ decreases as R_{C-C} increases. This feature is also apparent from the NPE, which is maximum at $R = 0.90\text{ Å}$ and minimum at $R = 3.00\text{ Å}$. It may be possible to obtain an even smoother potential-energy curve with a reduced NPE by the use of different CASs in the Franck-Condon and bonding regions,¹⁹ but this technically difficult problem is beyond the scope of the present straightforward test of standard approaches.

III. CONCLUDING REMARKS

We benchmark the ground and two low-lying singlet excited states of 1A_g symmetry (under the D_{2h} subgroup) for C_2 against the FCI and single-reference based CC methods and its variants. Most single-reference based calculations, including the CC treatments, yield quantitatively incorrect results, especially near the bond dissociation region as anticipated.

The computed error curve and the large NPE produced by single-reference based calculations indicate that bond breaking reactions cannot be modeled even by state-of-art single-reference based coupled cluster methods. The present work once again demonstrates that multireference approaches, such as the H^v method, are capable of producing highly reliable and uniformly accurate results even for such challenging systems as C₂, and, therefore, can be used to model the most difficult bond breaking/making reactions in both ground and excited states. While multireference methods are often criticized as scaling poorly with an increase in the size of the reference space, the present comparisons demonstrate once again^{15-17,19,20} that modest sized reference spaces suffice. Indeed, for “simpler” cases, such as two-dimensional potential surfaces for methyl mercaptan nonadiabatic photodissociation¹⁷ and three-dimensional surfaces for H₂S photodissociation,¹⁹ five orbital reference spaces appear quite suitable. Thus, the required size of the reference space does not scale with the size of the system but depends more on the complexity of its nondynamical correlation.

ACKNOWLEDGMENTS

The authors wish to thank Dr. M. S. Gordon and his group for providing their GAMESS code. This research is supported, in part, by PRF Grant No. 37939-AC7.

¹M. L. Abrams and C. D. Sherrill, J. Chem. Phys. **121**, 9211 (2004).

²F. Coester, Nucl. Phys. **7**, 421 (1958).

³F. Coester and H. Kümmel, Nucl. Phys. **17**, 477 (1960).

⁴J. Čížek, J. Chem. Phys. **45**, 4256 (1966).

⁵J. Čížek, Adv. Chem. Phys. **14**, 35 (1969).

⁶K. Raghavachari, G. W. Trucks, J. A. Pople, and M. Head-Gordon, Chem. Phys. Lett. **157**, 479 (1989).

⁷P. Piecuch, K. Kowalski, I. S. O. Pimienta, and M. J. McGuire, Int. Rev. Phys. Chem. **21**, 527 (2002), and references therein.

⁸P. Piecuch, K. Kowalski, P.-D. Fan, and I. S. O. Pimienta, in *Advanced Topics in Theoretical Chemical Physics*, Progress in Theoretical Chemistry and Physics Vol. 12, edited by J. Maruani, R. Lefebvre, and E. Brändas (Kluwer, Dordrecht, 2003), pp. 119–206, and references therein.

⁹D. Mukherjee and S. Pal, Adv. Quantum Chem. **20**, 291 (1989), and references therein.

¹⁰J. Paldus and X. Li, Adv. Chem. Phys. **110**, 1 (1999), and references therein.

¹¹K. F. Freed, *Lecture Notes in Chemistry* (Springer, Berlin, 1989), Vol. 52, p. 1.

¹²H. Sun, K. F. Freed, M. Herman, and D. L. Yeager, J. Chem. Phys. **72**, 4158 (1980).

¹³Y. S. Lee, H. Sun, M. G. Sheppard, and K. F. Freed, J. Chem. Phys. **73**, 1472 (1980).

¹⁴A. W. Kanzler, H. Sun, and K. F. Freed, Int. J. Quantum Chem. **39**, 269 (1991).

¹⁵R. L. Graham and K. F. Freed, J. Chem. Phys. **96**, 1304 (1992).

¹⁶C. M. Martin and K. F. Freed, J. Chem. Phys. **100**, 7454 (1994).

¹⁷J. E. Stevens, K. F. Freed, F. Arendt, and R. L. Graham, J. Chem. Phys. **101**, 4832 (1994).

¹⁸J. P. Finley and K. F. Freed, J. Chem. Phys. **102**, 1306 (1995).

¹⁹J. E. Stevens, R. K. Chaudhuri, and K. F. Freed, J. Chem. Phys. **105**, 8754 (1996).

²⁰R. K. Chaudhuri, A. Mudholkar, K. F. Freed, C. H. Martin, and H. Sun, J. Chem. Phys. **106**, 9252 (1997), and references therein.

²¹J. P. Finley, R. K. Chaudhuri, and K. F. Freed, J. Chem. Phys. **103**, 4990 (1995); Phys. Rev. A **54**, 343 (1996); R. K. Chaudhuri, J. P. Finley, and K. F. Freed, J. Chem. Phys. **106**, 4067 (1997).

²²A. Dutta and C. D. Sherrill, J. Chem. Phys. **118**, 1610 (2003).